JICS

CSURE 2014 Summer Program

Modeling the Effects of Increased Glucose Concentration on Intraocular Pressure

Author:
Caroline Su
(University of California, Berkeley)
Alexander Cope
(Centre College)
Contributor:
Ben Ramsey
(University of Tennessee, Knoxville)

Supervisor:
Dr. Kwai Wong
(University of Tennessee, Knoxville)

August 8th, 2014

Abstract

Glaucoma is one of the leading causes of blindness in the world. Two of the known risk factors for glaucoma development are high fluid pressure within the eye and diabetes. We have developed a model which relates aqueous humor flow in the anterior chamber of the eye to increased glucose concentration. Our ultimate goal is to develop this model and perform simulations in 3D using FEATool and Deal.II and obtain consistent results. Currently, standard Navier-Stokes flow has been modeled successfully and consistently using FEATool and Deal.II in 2D. The simulations are in the process of being expanded to run in 3D. From there, the modified equations can be incorporated into the simulations.

1 Introduction

Despite its small size, the human eye is a complex organ which has demanded the attention of researchers for centuries. The eye is made up of three main chambers: the anterior chamber, the posterior chamber, and the vitreous chamber. The anterior chamber (located between the cornea and the iris) contains the aqueous humor, a clear, water-like fluid which will be the focus of this study. The aqueous humor distributes nutrients to the anterior part of the eye and regulates the intraocular pressure (IOP). The aqueous humor is continuously produced in the ciliary body and is released into the anterior chamber. From there, the fluid travels through the trabecular meshwork, a matrix like structure, and then into the Schlemms canal, where the aqueous humor mixes with venous blood. This pathway accounts for the majority of aqueous outflow. The trabecular meshwork and Schlemms canal are considered to be the main contributors to resistance to aqueous outflow.

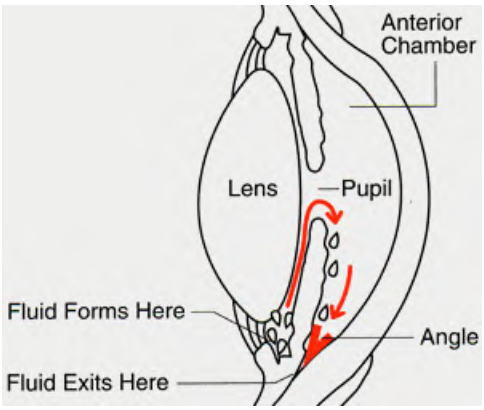

Figure 1: http://www.theeyecenter.com/educational/005.htm

Increased IOP has been well-documented as a risk-factor for the development of glaucoma, the 2nd leading cause of blindness in the United States. IOP is thought to normally increase due to one of two main causes: an increased resistance to aqueous flow within the trabecular meshwork and the Schlemms canal, which would result in open-angle glaucoma;

Porosity (ϵ)	Permeability (m^2) of TM	Pressure in AC (Pa)
0.4	7.59×10^{-14}	1271
0.3	2.35×10^{-14}	1429
0.25	1.19×10^{-14}	1655
0.225	8.09×10^{-15}	1867
0.2	5.33×10^{-15}	2211
0.175	3.36×10^{-15}	2805
0.15	1.99×10^{-15}	3905
0.125	1.09×10^{-15}	6154
0.1	5.27×10^{-16}	11437

Table 1: Effects of decreased porosity on IOP[3]

κ	AvgPreAC	AvgPreTM	$\triangle Pre$
2×10^{-05}	-2.1230×10^{-1}	-2.9939×10^{0}	2.7816×10^{0}
2×10^{-06}	-5.7427×10^{-2}	-2.4961×10^{1}	2.4904×10^{1}
2×10^{-07}	1.4873×10^{0}	-2.4463×10^{2}	2.4314×10^{2}
2×10^{-08}	1.6932×10^{1}	-2.4410×10^{3}	2.4241×10^{3}
2×10^{-09}	1.7138×10^{2}	-2.4404×10^{4}	2.4233×10^{4}

Table 2: Permeability of trabecular meshwork and relation to IOP. κ represents permeability and $\triangle P$ represents the overall change in IOP [2]

or the sudden moving forward of the iris, closing the gap through which the aqueous humor exits the anterior chamber, which is known as closed-angle glaucoma.

As a result of the relatively high frequency of glaucoma diagnoses, many researchers have sought to model changes in IOP as a result of aqueous humor flow. Recently, a model developed by J.A. Ferreira et. al. [3] simulated 2D flow of the the aqueous humor and its relation to both obstruction of the trabecular meshwork and as a form of drug distribution. They found that, as expected, increased obstruction of the trabecular meshwork (modeled by decreasing the porosity parameter in Darcys Law) resulted in increased IOP.

Similarly, Crowder and Ervin [2] developed an axisymmetric model using both Navier-Stokes and Darcys Law. As expected, they found that permeability and IOP were inversely proportional; with each order of magnitude that permeability decreased, IOP increased by the same order of magnitude (see Table 2).

Experimental studies indicate the role of temperature changes in aqueous humor flow [4]. When an eye is open, a temperature gradient is established between the cornea (approximately outside temperature) and the iris/lens (approximately normal body temperature). This temperature gradient establishes buoyancy driven flow, which was modeled by both Canning et. al[1] and Fitt and Gonzalez[4]. These models revealed the dominant effect of buoyancy driven flow over other forces, with flow speeds being of order 0.1 mm/s.

When temperature is uniform within the anterior chamber, buoyancy-driven flow is minimal, causing the main driving force to be flow of aqueous humor through the pupil aperture. In simulations run by Fitt and Gonzalez[4], maximum flow velocity was found to be near $7.5 \times 10^{-}6^{m}/_{s}$.

Previous studies have also found a strong correlation between those affected by diabetes and the development of glaucoma. While the exact mechanism resulting in the development of glaucoma due to diabetes in unknown, research completed by Tsuyoshi Sato and Sayon Roy[6] found that fibronectin production in the trabecular meshwork does increase in high-glucose concentration environments. It is believed this increase in fibronectin results in an increased resistance to flow of the aqueous humor out of the anterior chamber of the eye.

2 Objective

The ultimate goal of our model is to simulate IOP under both normal glucose concentration and high glucose concentrations. We will model human eyes under different situations: with all other factors remaining constant, let glucose concentration be the experimental factor, starting with that of an average adult ($5.5^{mmol}/_{L}$) and increase to that of an adult with type 2 diabetes ($8^{mmol}/_{L}$). Then we will compare the results of calculated IOP and discuss the correlation between diabetes and glaucoma. It is expected that as glucose concentration increases, IOP will also increase. If successful, this model could provide insight as to why diabetics are at a higher risk of developing open-angle glaucoma.

We will also attempt to develop our own software which will solve our systems of equations. The software will be designed to run in parallel using MPI and Trilinos software packages. The code will initially be designed to solve the Laplace equation,

$$\triangle u = 0 \tag{1}$$

Once this code has been made to work for 1D and 2D, it will then be expanded to fit the equations of our model. By developing a program that can solve these equations in parallel across many processes, simulations can be performed on more refined meshes in a faster amount of time.

3 Methods

The models we have developed borrows significantly from previous 2D and 3D models of aqueous humor flow. Many of the equation used were borrowed and modified from the 3D model used by Adan Villamarin et. al.[7]. The cornea will be modeled as a rigid structure, allowing the no-slip boundary condition to be used. The iris will also be considered as a rigid structure, although the model may later be expanded to treat the iris as a linearly elastic structure[5]. The pupil aperture will be treated as the inlet with a radius of 8 mm through which the aqueous humor enters the anterior chamber, but its size and shape will remain constant throughout the simulation. The eye will be positioned such that to model

flow when a person is standing and looking forward (see Figure 1). The aqueous humor will flow into the anterior chamber with an initial velocity of 1.2 mm/s (J.A Ferreira et al)[3].

The fluid flow in the anterior chamber (which will be 3mm wide between the cornea and the pupil aperture) will be modeled using a modified form of the Navier-Stokes equations for incompressible flow, which includes an additional term for thermal change:

$$\rho\bar{v} \cdot \bigtriangledown\bar{v} = - \bigtriangledown p + \mu \bigtriangledown^2 \bar{v} + rho_0\bar{g}\beta(T - T_{ref}) \tag{2}$$

The equations below describes the continuity that aqueous humor for steady and incompressible flow has to satisfy in the anterior chamber:

$$\bigtriangledown \cdot \bar{v} = 0 \tag{3}$$

And the equation below describes the convective and diffusive transport of energy by aqueous humor where viscous dissipation effect has been neglected:

$$\rho C_p\bar{v} \cdot \bigtriangledown T = k \bigtriangledown^2 T \tag{4}$$

where k is the thermal conductivity and C_p is the heat capacity. This modified set of equations reflects the buoyancy-driven nature of aqueous humor flow.

In order to simplify the model, the trabecular meshwork and Schlemms canal will be treated as a uniform porous region over. The initial outflow pressure will be treated as 1200 Pa[3] This will allow the permeability of the trabecular meshwork and Schlemms canal to be modeled using a modified form of Darcys law which accounts for fibronectin production:

$$\alpha = {}^{\mu}/_{\triangle p} \triangle e\bar{v} - f(g_c) \tag{5}$$

where $\triangle e$ is the thickness of the porous domain and $f(g_c)$ represents the fibronectin function, and g_c is the given glucose concentration (in mg/dL). As the rate of fibronectin production within the trabecular meshwork is unknown, we assume this value can be modeled by the ODE:

$${}^{df}/_{dg_c} = rg_c \tag{6}$$

where $r > 0$. This ODE can be solved using separation of variables to yield:

$$f(g_c) = {}^{1}/_{2}r(g_c)^2 + C \tag{7}$$

where C is some constant.

The PDEs will be solved using Finite Element Method software. Initial tests will be performed using a 2D model created in Cubit and imported into the FEATool software (see Figure 2). Once the model has been fine-tuned, the model will be expanded into a 3D model displaying the relevant portions of the eye. This mesh will also be created using the Cubit software and will be solved using the deall.II programs. Finally, the simulations will be run in a parallel environment on the Darter Cray XC30 system found at the Oak Ridge National Laboratory. This supercomputer has a peak performance of 250 TeraFLOPS (10^{12} floating point operations per second).

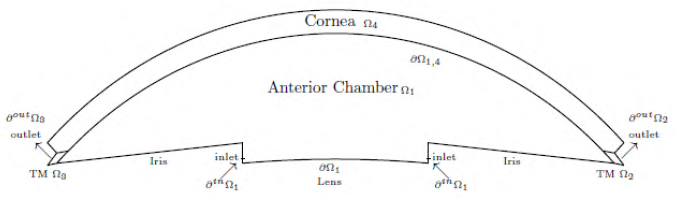

Figure 2: 2D model of the human eye[3]

Parameter	Value
Initial Velocity (v_0)	$1.2\ ^{mm}/_{s}$
Outlet Pressure (p_0)	1200 Pa
Reference Temperature (T_{ref})	22 °C
Aqueous Humor Density (ρ)	$1000^{kg}/_{m^3}$ (water property)
Aqueous Humor Viscosity (μ)	$0.001^{kg}/_{m\cdot s}$ (water property)
Aqueous Humor Specific Heat (C_p)	$4182^{J}/_{kg\cdot K}$ (water property)
Aqueous Humor Thermal Conductivity (k)	$0.6^{W}/_{m\cdot K}$
Glucose Concentration (g_c)	$99.1001^{mg}/_{dL}$ (healthy eye)
	$144.1456^{mg}/_{dL}$ (type 2 diabetic eye)

4 Results

A 2D Cubit-generated mesh representing the anterior chamber portion of the eye was imported into the FEM solver. The simulation was run using a low Reynolds number (Re=1.2), 0.12 as the inlet velocity, and 9.4 as the outlet pressure. The results were output in a .vtk format in order to view them using VisIt software. It is important to note that these initial results do not include flow out of the trabecular meshwork. Instead, small regions near the edges of the anterior chamber were selected as the outflow area.

Figure 3: normal eye: 2D velocity

The effects of a higher Reynolds number were also assessed. Figure 4 shows the results of flow using the same values for velocity and pressure, but with Re = 2.5

Both a low resolution and a high resolution 3D mesh was generated in Cubit. Boundary conditions were set up to be consistent with those established in the 2D simulations. The same initial conditions and Reynolds number were also used for the simulations. Initial 3D simulations were run using the low resolution mesh due to computational complexity of

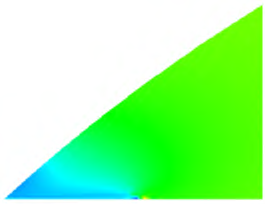

Figure 4: normal eye: 2D pressure

Figure 5: normal eye: 2D velocity (Re=2.5)

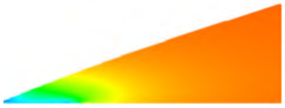

Figure 6: normal eye: 2D pressure (Re=2.5)

simulating 3D fluid flow. The results can be seen in Figure 10. In order to obtain more accurate results, a simulation was run using the more refined mesh. The results can be seen in Figure 7, 8 and 9.

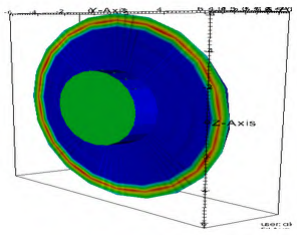

Figure 7: normal eye: 3D velocity

The 1D Laplace solver was run using 5 global elements with the values of u at boundary nodes 0 and 4 being 0 and 100, respectively. The expected values of the inner 3 nodes are 25, 50, and 75, which were the results obtained by our 1D Laplace solver. The output of the code can be seen below.

```
Lapalce 1D Solver output with 5 global elements and 3 processors:

Epetra::CrsMatrix
Number of Global Rows     = 5
```

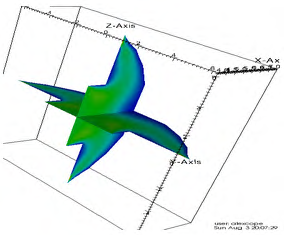

Figure 8: normal eye: 3D velocity (sliced)

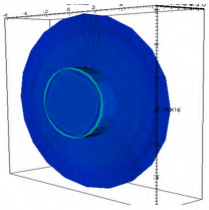

Figure 9: normal eye: 3D relative pressure

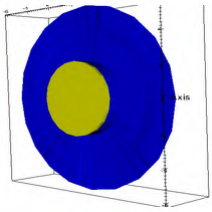

Figure 10: normal eye: 3D velocity (low resolution)

```
Number of Global Cols     = 5
Number of Global Diagonals = 5
Number of Global Nonzeros = 13
Global Maximum Num Entries = 3

Number of My Rows      = 2
Number of My Cols      = 3
Number of My Diagonals = 2
Number of My Nonzeros  = 5
My Maximum Num Entries = 3

Epetra::CrsMatrix
Number of My Rows      = 2
Number of My Cols      = 4
Number of My Diagonals = 2
Number of My Nonzeros  = 6
My Maximum Num Entries = 3
```

```
Epetra::CrsMatrix
Number of My Rows      = 1
Number of My Cols      = 2
Number of My Diagonals = 1
Number of My Nonzeros  = 2
My Maximum Num Entries = 2

       Processor      Row Index      Col Index      Value
       0                      0                      0                      1
       0                      0                      1                      0
       0                      1                      0                      -1
       0                      1                      1                      2
       0                      1                      2                      -1
       1                      2                      2                      2
       1                      2                      3                      -1
       1                      2                      1                      -1
       1                      3                      2                      -1
       1                      3                      3                      2
       1                      3                      4                      -1
       2                      4                      4                      1
       2                      4                      3                      0

              *******************************************************
              ***** Problem: Epetra::CrsMatrix
              ***** Preconditioned GMRES solution
              ***** Order 1 Neumann series polynomial
              ***** No scaling
              *******************************************************

              iter:   0                   residual = 1.000000e+00
              iter:   1                   residual = 4.515050e-01
              iter:   2                   residual = 1.814261e-01
              iter:   3                   residual = 3.162662e-04
              iter:   4                   residual = 1.048770e-35


              Solution time: 0.000562 (sec.)
              total iterations: 4
Solved x: Epetra::Vector     MyPID          GID            Value
                             0              0              0
                             0              1              25
Solved x: Epetra::Vector     1              2              50
                             1              3              75
Solved x: Epetra::Vector     2              4              100
```

A 2D geometry of the anterior chamber area of human eye is created within FEATool software, then boundary conditions are added on different regions/sections. Inflow is set to be the from the pupil area, and outflow (without trabecular meshwork area) is set at the end points of anterior chamber. Mesh generation and calculation can also be performed within the software. The results are shown below:

Figure 11: normal eye: 2D velocity

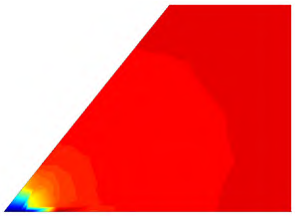

Figure 12: normal eye: 2D pressure

From the graphs, we can note that velocity is fairly consistent throughout the anterior chamber region, and the dramatic change in outflow regions is due to their relative small sizes. The intraocular pressure also remains consistent throughout the whole region except the changes that occur near the outflow area.

Since the results of 2D simulation fit the expectations, we expand the simulation onto 2D axis-symmetric model. A geometry that resembles half of the anterior chamber, along with the addition of trabecular meshwork and Schlemms canal, is created. In addition to the application of standard Navier-Stokes equation, Darcys law is also applied on the Schlemms canal area. Then simulation in 2D was performed on the model and result can be displayed in the 3D geometry created by rotating the model around the axis (center of anterior chamber). The results from 2D axis-symmetric model are shown below:

The results from 2D and 2D axis-symmetry are consistent, with relative consistent speed and pressure throughout anterior chamber region and dramatic changes in outflow region. However, the Darcys law seems to have little to no effect on intraocular pressure. Although we were unable to figure out the reasons behind it, we manually modified the inflow pressure to perform simulations to observe the fluid flow in glaucoma eye.

And a rough 3D model also shows similar result for velocity.

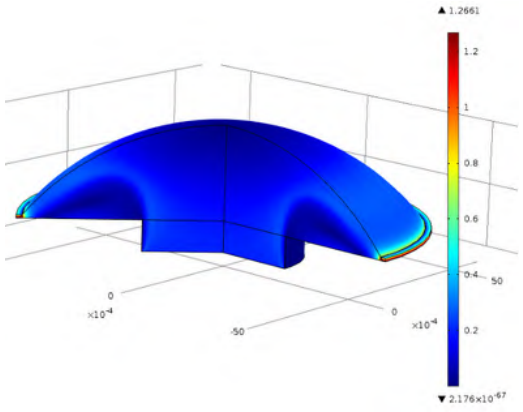

Figure 13: normal eye: 2D axis symmetry velocity

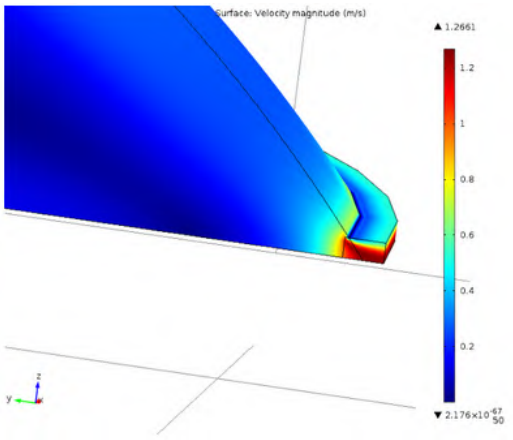

Figure 14: normal eye: 2D axis symmetry velocity (detail)

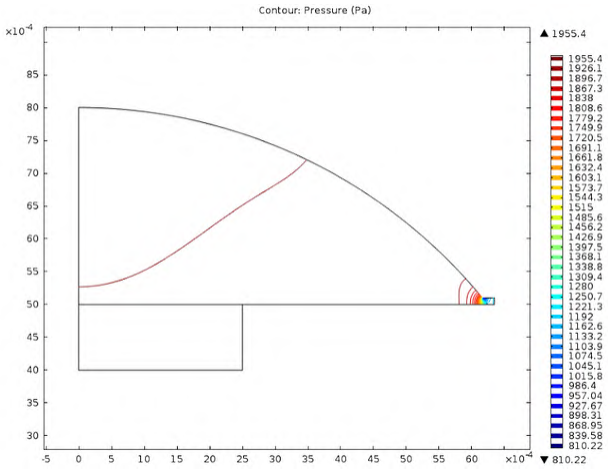

Figure 15: normal eye: 2D axis symmetry pressure

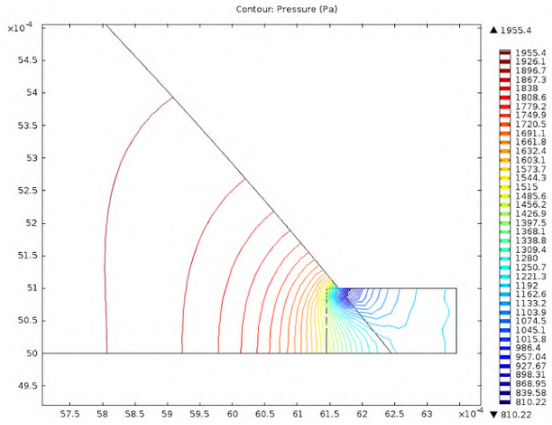

Figure 16: normal eye: 2D axis symmetry pressure (detail)

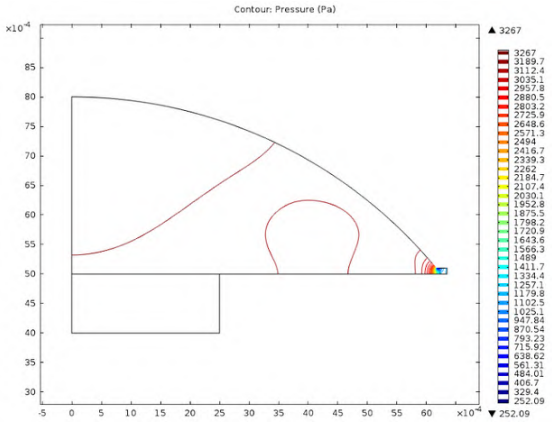

Figure 17: glaucoma eye: 2D axis symmetry pressure

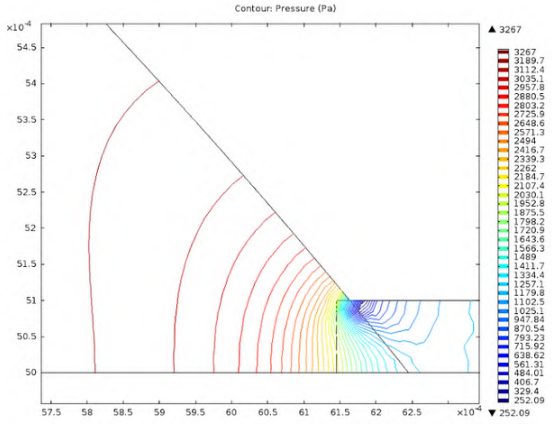

Figure 18: glaucoma eye: 2D axis symmetry pressure (detail)

5 Conclusions and Future Work

When comparing 2D simulations performed in FEATool and Deal.II, the flow of the aqueous humor appears to be relatively consistent. The velocity stays relatively constant throughout the anterior chamber except when it begins to approach the outlet boundaries. At this point, a dramatic increase in velocity is seen. The pressure results are consistent in the sense that a decrease in pressure is seen close to the outlet regions, but it appears that FEATool indicates the pressure is higher in the anterior chamber than Deal.II. The cause of these inconsistencies in pressure will require further investigation.

One thing that became apparent rather quickly was the effect of using a low resolution versus a high resolution mesh in Deal.II. Due to the lengthy time of 3D simulations, low resolution meshes were initially used. This allowed the 3D simulations to complete within approximately 30 to 40 minutes. However, compared to simulations run in FEATool, these results were quite inaccurate. When a simulation was run using a slightly more refined mesh, the velocity plot was much more consistent with 3D results in FEATool. The tradeoff was this more refined mesh required a significant amount of time to complete compared to the 2D simulations. Ultimately, it was determined more accurate results were more important than the time lost by using a refined mesh. The issue of lengthy run times is not unsolvable. Deal.II programs can run in parallel using Trilinos and MPI, barring that Deal.II is linked to these packages during the build process. If the sparse matrices and vectors can be distributed amongst several processors, the run time of the 3D simulations will be reduced significantly.

At this point, we have mainly modeled fluid flow within the anterior chamber using the standard Navier-Stokes equations. A region was added in FEATool meant to represent the trabecular meshwork, but the results from these simulations did not result in any changes to the flow of aqueous humor. These results were inconsistent with the results of Ferreira et al., meaning further modifications will need to be made to the current FEATool model.

The 1D Laplace parallel solver is at the point where it can be expanded to 2D and 3D. This will require numerous extra features, although the general structure of the code is the same. While a 1D Laplace problem can only be applied over a set of nodes distributed over a line, a 2D/3D Laplace problem could be distributed over a variety of meshes. A function will need to be created to read in the file and establish the offsets and column locations. It will also require a more complicated local matrix setup as the values will vary from local element to local element.

References

[1] C.R. Canning, *Fluid Flow in the Anterior Chamber of a Human Eye.* Mathematical Medicine and Biology, 19.1, 31-60, 2002

[2] T.R.Crowder and V.J. Ervin, *Numerical Simulations of Fluid Pressure in the Human Eye.* Applied Mathematics and Computation, 219.24, 11119-11133, 2013.

[3] J.A. Ferreira, P. de Oliveira, P.M. da Silva and J.N. Murta *Numerical Simulation of Aqueous Humor Flow: from Healthy to Pathologic Situations*. Applied Mathematics and Computation, 226, 777-792, 1994.

[4] A.D. Fitt and G. Gonzalez, *Fluid Mechanics of the Human Eye: Aqueous Humour Flow in the Anterior Chamber*. Bulletin of Mathematical Biology, 68.1, 53-71, 2006.

[5] J.J. Heys, V.H. Barocas and M.J. Taravella, *Modeling Passive Mechanical Interaction between Aqueous Humor and Iris*. Journal of Biomechanical Engineering, 123.6, 540, 2001

[6] S. Roy, R. Kao and T. Sato, *Effect of High Glucose on Fibronectin Expression and Cell Proliferation in Trabecular Meshwork Cells*. Investigative Ophthalmology and Visual Science, 43.1, 170-175, 2002.

[7] A. Villamarin, S. Roy, R. Hasballa, O. Vardoulis, P. Reymond and N. Stergiopulos, *3D Simulation of the Aqueous Flow in the Human Eye*. Medical Engineering and Physics, 34.10, 1462-1470, 2012.